Analytical and Bioanalytical Chemistry (2021) 413:1521–1532
https://doi.org/10.1007/s00216-020-03135-0

PAPER IN FOREFRONT

A precise and rapid isotopomic analysis of small quantities of cholesterol at natural abundance by optimized ^{1}H-^{13}C 2D NMR

Lenny Haddad[1,2] · Sophie Renou[1] · Gérald S. Remaud[1] · Toufic Rizk[2] · Joseph Bejjani[2] · Serge Akoka[1]

Received: 2 November 2020 / Revised: 15 December 2020 / Accepted: 16 December 2020 / Published online: 27 January 2021

Abstract

Cholesterol, the principal zoosterol, is a key metabolite linked to several health complications. Studies have shown its potential as a metabolic biomarker for predicting various diseases and determining food origin. However, the existing INEPT (insensitive nuclei enhanced by polarization transfer) ^{13}C position-specific isotope analysis method of cholesterol by NMR was not suitable for very precise analysis of small quantities due to its long acquisition time and therefore is restricted to products rich in cholesterol. In this work, a symmetric and adiabatic heteronuclear single quantum coherence (HSQC) 2D NMR sequence was developed for the high-precision (few permil) analysis of small quantities of cholesterol. Adiabatic pulses were incremented for improving precision and sensitivity. Moreover, several strategies such as the use of non-uniform sampling, linear prediction, and variable recycling time were optimized to reduce the acquisition time. The number of increments and spectral range were also adjusted. The method was developed on a system with a cryogenically cooled probe and was not tested on a room-temperature system. Our new approach allowed analyzing as low as 5 mg of cholesterol in 31 min with a long-term repeatability lower than 2‰ on the 24 non-quaternary carbon atoms of the molecule comparing to 16.2 h for the same quantity using the existing INEPT method. This result makes conceivable the isotope analysis of matrices low in cholesterol.

Keywords Cholesterol · Quantitative NMR · 2D HSQC · ^{13}C isotope analysis · Isotopomics

Introduction

Cholesterol is an essential membrane constituent of mammalian cells and has an important role in cellular organization and stability. Cholesterol also plays an important role as a precursor of steroid hormones, vitamin D, oxysterols, and bile acids [1]. It is implied in many health problems [2–4] and has proven to be an important metabolic biomarker [5, 6] since the profile of steroid hormones was important in clinical diagnostics [7].

It was shown that the global content in ^{13}C (isotope composition: $\delta^{13}C_g$) of cholesterol present in human bones mirrors the most recent diet of the individual [8–11]. This parameter is currently obtained by isotope ratio measured by mass spectrometry (irm-MS, also known as IRMS [isotope ratio by mass spectrometry]) [12]. However, irm-MS only has access to the average isotopic composition, which is the mean value of the ^{13}C content within the considered molecule. As a result, information of the coexistence of both normal and inverse ^{13}C isotope effects during the biosynthesis of cholesterol is indubitably lost. In this respect, it is also known that the processes affecting the carbon isotopic composition of isoprenoid lipids would be better elucidated by an intramolecular ^{13}C composition study [13]. Position-specific isotope analysis (PSIA) can be achieved by several approaches such as (bio)chemical degradations or pyrolysis but with limited applications (only small molecules and/or partial intramolecular information and/or tedious protocols) [14–16]. Recently, analyses of molecular isotopic structure have been proposed by tandem mass spectrometry, using an Orbitrap mass analyzer [17–20]. However, in the level of the current development, these methodologies seem promising, but only for small molecules. But, irm-NMR (isotope ratio measured by nuclear magnetic resonance) is not limited by the molecular weight [21]. Isotopic analysis by ^{2}H-NMR was used to identify exogenous sources of sugars in wine by analyzing

✉ Serge Akoka
Serge.akoka@univ-nantes.fr

[1] CNRS, CEISAM UMR 6230, Faculté des Sciences, Université de Nantes, BP 92208, 2 rue de la Houssinière, 44000 Nantes, France

[2] Research Unit: Technologies et Valorisation Agroalimentaire (TVA), Laboratory of Metrology and Isotopic Fractionation, Faculty of Science, Saint Joseph University of Beirut, Mar Mikhael, P.O. Box 17-5208, Beirut 1104 2020, Lebanon

the D/H ratio of many compounds [22, 23] (the SNIF-NMR™ method). Profiling of intramolecular ^{13}C contents by means of irm-^{13}C NMR was not straightforward because of the high level of precision required. Indeed, the variations of the quantity of ^{13}C isotopomers are very low in nature: to observe ^{13}C isotopic fractionation, a precision of the order of 1‰ (0.1%) has to be reached by the analytical method used. Only in the last 12 years has a full protocol been proposed to achieve such a performance [24]. Irm-^{13}C NMR was then used in various domains [25–27]. Recently, irm-NMR took advantage of the multi-pulse sequences available for the ^{13}C nucleus to improve sensitivity and/or resolution but still keep the high precision as the analytical target, as demonstrated by the analyses of ^{13}C position-specific isotope composition (PSIA) of triglycerides [28, 29]. In a previous study, 90 mg of cholesterol was necessary to reach the high precision requested for isotopomic measurements using an optimized INEPT (insensitive nuclei enhanced by polarization transfer) sequence [29]. That was already challenging in terms of molecule size and NMR tube concentration since a high signal-to-noise ratio (SNR) was required in order to obtain a precision of 1‰ in a relatively short analysis time [30, 31].

So far, compound-specific isotope analysis (CSIA) by gas chromatography coupled to irm-MS [32, 33] is the only method enabled to work with few milligrammes of products. None of the previously proposed irm-NMR approaches can cope with limitations regarding the cholesterol quantity and the NMR acquisition time. Indeed, the main issue remains sensitivity. In a recently published methodology, ^{1}H NMR was used for determining position-specific $^{13}C/^{12}C$ ratios within organic [34]. The main advantage of this approach is the sensitivity intrinsic to proton-detected NMR experiments, but no overlapping of ^{1}H signals is required. That is not the case for cholesterol as illustrated in Fig. 1 even at high field as with the 700-MHz spectrometer used here.

Therefore, to the best of our knowledge, today there is no method to perform a quantitative analysis of a few milligrammes of cholesterol with the precision required by isotopic measurements (permil), and so, a new methodology has to be proposed. In this respect, the heteronuclear single quantum coherence (HSQC) spectroscopy experiment has proven to be an effective method to quantify metabolites in complex mixtures [35, 36]. Our group recently developed a HSQC pulse sequence with perfect radiofrequency (RF) symmetry and successfully applied this new sequence to triglyceride matrices [37].

The aim of this study was to develop an HSQC method for small quantities of cholesterol able to quantitate ^{13}C isotopic contents of protonated carbon centres in this molecule with a precision of a few permil (‰). Thus, cholesterol isotopomics could be applied to matrices such as dairy products. The questions are then as follows: (i) what changes must be made to the core of the HSQC multi-pulse sequence? (ii) What parameters must be adjusted to reach the targeted precision? And (iii) what is the minimum amount of cholesterol needed to reach the target precision (‰) with an analysis time lower than 1 h? The key to answering these questions was based on the inclusion of special adiabatic RF pulses which when implemented properly result in the prerequisite gain in precision and sensitivity. Moreover, several factors such as the use of variable recycling times (VRT) [38], non-uniform sampling (NUS) [39], and linear prediction (LP) [40] were evaluated and optimized in order to reduce the NMR experiment duration. Additionally, the number of t_1 increments and spectral range were also adjusted [41]. Also included is a comment on the nature of the data obtained and their relation to the isotopomics concept at natural abundance.

Experimental section

Chemicals

Extra pure ethanol and petroleum ether (boiling range 308–333 K, ACS basic) were purchased from Scharlab; diethylether (GPR Rectapur) and methanol (AnalaR Normapur) were purchased from VWR chemicals; potassium hydroxide (ACS reagent, ≥ 85%) was purchased from Sigma-Aldrich; and deuterated chloroform was purchased from Eurisotop. Whatman Purasil silica gel (60A, 230e400 Mesh ASTM) was used for column chromatography. Commercial cholesterol (Δ^5-Cholesten-3-ol) was purchased from Sigma Grade (99+ %).

Cheese samples

Four cheese samples of French origin were purchased from grocery stores. Samples consist of Emmental (sample 1), Pyrenean cheese (sample 2), and Comté (samples 3 and 4).

Cheese cholesterol extraction

In this work, a specific procedure was developed for the quantitative extraction of cholesterol in cheese samples. Unless otherwise specified, working temperature was 295 ± 1 K. Cheese samples (30 g) were taken from the middle of the cheese blocks. Samples were cut in small pieces and dissolved in absolute ethanol (60 mL on average, depending on samples) at a temperature between 313 and 323 K. The mixture was then filtered after 15 min of protein precipitation, and the residue washed with petroleum ether (70 mL), ethanol:diethylether (1:1 v/v, 30 mL), and diethylether (60 mL). Complete extraction of lipids was assessed by thin-layer chromatography (TLC). Solvents were evaporated under vacuum at 318 K. The precipitate appearing during the concentration of the solution was separated by decantation of the liquid phase containing total

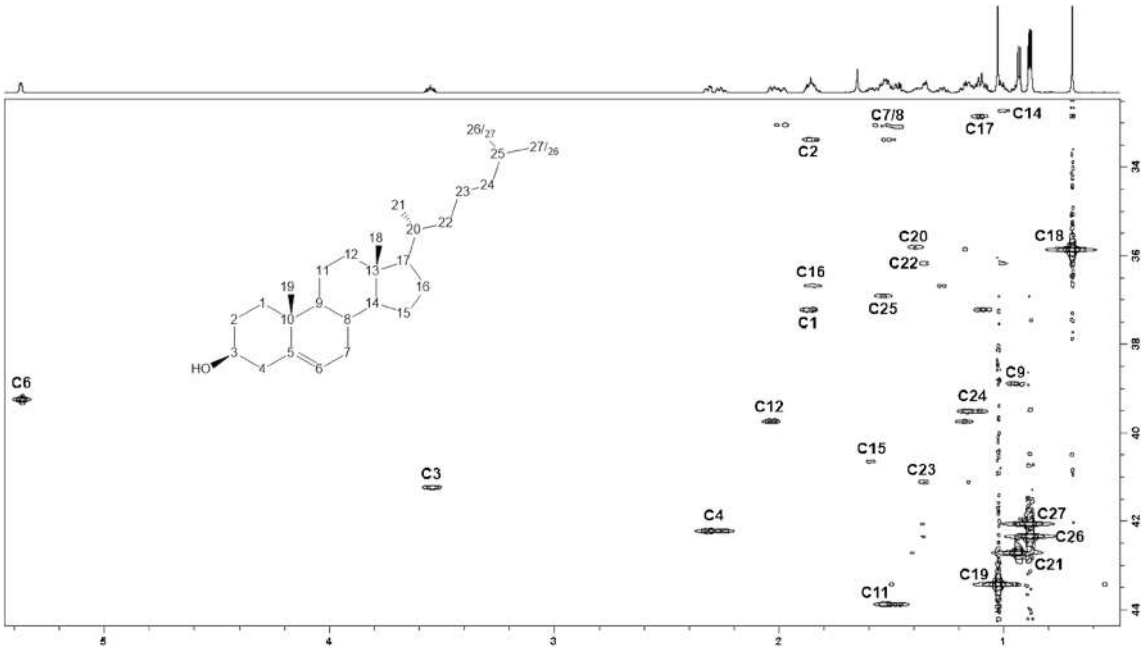

Fig. 1 HSQC spectrum from 10 mg of cholesterol recorded at 700.28 MHz with a cryoprobe in 31 min, using the spectral aliasing approach: small spectral width (12 ppm) in the F_1 dimension (^{13}C) with 50% NUS and TD = 512. Sample temperature was set at 288 K. Note on the top the ^{1}H NMR spectrum of cholesterol with severe overlapping

lipids. The precipitate was washed with absolute ethanol (3 × 10 mL) and then with diethylether (10 mL). Washing fractions and the liquid phase containing extracted lipids were combined and evaporation of solvents continued. Total lipids (8.5 g) thus obtained were subjected to a solid-phase extraction (SPE) over 7.8 g of silica gel to separate triacylglycerols and cholesterol. Lipids were dissolved in 40 mL of diethylether:petroleum ether (1:9 v/v) and pulled through the column. Additional 85 mL was necessary to elute triacylglycerols (TAG). Diethylether (35 mL) was used to elute cholesterol. Solvent in the fraction containing cholesterol was evaporated under vacuum at 318 K. The residue was dissolved in 1.2 mL of diethylether, distilled water (0.16 g) and a solution of potassium hydroxide in methanol (2 N, 1.2 mL) were added, and the mixture was stirred during 30 min at 318 K in order to hydrolyze the remaining acylglycerols. The liquid phase of the reaction mixture was then filtered through 1 g of silica gel, and 40 mL of diethylether was used to completely elute cholesterol and free fatty acids. After solvent evaporation (under vacuum at 308 K), the residue was dissolved in diethylether:petroleum ether (1:9 v/v, 0.5 mL) and added onto a column chromatography (2 g silica gel). Fatty acids were eluted using 35 mL of diethylether:petroleum ether (1:9 v/v). Cholesterol was then eluted with 38 mL of diethylether:petroleum ether (1:3 v/v) and solvents evaporated as in the previous step. Typically, a mixture containing approximately 25 mg of cholesterol and 6 mg of fatty acids was obtained, which implies a cholesterol purity greater than 80%, as assessed by ^{1}H NMR. It can be noted that other methods and notably that proposed by Srivastava et al. [42] could be used to extract cholesterol.

NMR sample preparation

Requested quantity of commercial cholesterol (20, 10, or 5 mg) was dissolved in 600 μL of chloroform-d_1 in order to obtain a concentration of 33.3 mg mL^{-1} (86.2 mmol L^{-1}), 16.65 mg mL^{-1} (43.1 mmol L^{-1}), and 8.83 mg mL^{-1} (21.55 mmol L^{-1}), respectively. Cheese cholesterol samples (approx. 25 mg) were dissolved in the same volume of chloroform-d_1. Solutions thus obtained were carefully filtered into 5-mm high-quality NMR tubes.

NMR acquisition parameters

NMR experiments were performed on a Bruker Avance III HD 700 spectrometer equipped with an inverse $^{1}H/^{13}C/^{15}N/^{2}H$ cryogenically cooled probe carefully tuned to the recording frequency of 176.09 MHz for the ^{13}C and to 700.28 MHz for the ^{1}H. The sample temperature was set at 288 K.

^{1}H and ^{13}C RF powers were carefully adjusted in order to obtain 90° pulse widths equal to 10 μs and 11 μs, respectively, with an acquisition time of 0.1 s, recovery time of 10 s (the longest ^{1}H T_1, T_1^{max} = 1.4 s, was measured for the proton borne by the carbon C3; see Fig. 1

for carbon numbering), 8 dummy scans, and 2 scans. ^{13}C and ^{1}H offsets were set at 37 ppm and 4 ppm, respectively. Evolution period (Δ) was adjusted to 2.3 ms. Adiabatic full-passage pulses were designed with a cosine amplitude modulation of the radiofrequency (RF) field (ω_1^{max} = 157.1 kHz and 93.89 kHz for ^{13}C and ^{1}H, respectively) and frequency sweep derived from the amplitude shape using an offset-independent adiabaticity algorithm with an optimized frequency sweep ΔF (ΔF = 39 kHz and 17 kHz for ^{13}C and ^{1}H, respectively) as described in [43]. For inversion pulses, adiabatic full-passage pulses were used. For refocusing pulses, adiabatic composite pulses were applied [44]. ^{1}H decoupling was performed using an optimized phase cycle and adiabatic full-passage RF pulses with a cosine square amplitude modulation (ω_2^{max} = 110.6 kHz) and offset-independent adiabaticity with an optimized frequency sweep (ΔF = 14 kHz) as described in [43].

Purge gradients were set to g_0 = 25 G cm^{-1}, g_1 = 40 G cm^{-1}, and g_3 = 20 G cm^{-1}, while coherence order selection was obtained by g_2 = 40 G cm^{-1} and g_4 = 10.05 G cm^{-1}. Duration of all gradient pulses was 1 ms (excepted for g_0 whose duration was 10 ms) followed by a recovery delay of 300 μs.

Spectra were acquired with 512 t_1 increments and with 50% of compression rate from an NUS scheme.

NMR processing and integration parameters

NMR spectra were processed using the TopSpin 4.0.5 software. Before Fourier transform, cosinusoidal and trapezoidal functions (TM_1 = 0 and TM_2 = 0.5) were applied in dimension F_2 and F_1, respectively. The data matrices were zero-filled to 8192 points in F_2 and 2048 points in F_1. An automatic polynomial baseline correction (n = 2) was achieved in each direction for all the spectra.

Integration of 2D peak volumes was performed using the Topspin 4.0.5 software. As integration limits affect the results obtained, they were carefully chosen to be the same for all the peaks. They were defined to correspond—in both sides and in F_1 and F_2 dimensions—to 5% of the maximum signal intensity (see Supplementary Information (ESM) Fig. S1). In order to have the same integration volumes, all the spectra were calibrated in frequency. Calibration was adjusted on carbon 6 (5.36 ppm in F_2 and 39.23 ppm in F_1), which does not overlap with other carbons. Three spectra were recorded per session and each spectrum was processed three times (mainly to compensate for spectral alignment imperfections), leading to nine values for each measurement. Reconstruction of the 2D spectrum was performed using CS algorithms within TopSpin.

Molar fractions

Molar fraction was the parameter used to define the relative intramolecular ^{13}C distribution within cholesterol. Molar fraction (f_i) on each position i was calculated from peak volumes (V_i) using:

$$f_i = \frac{V_i}{\sum_1^n V_i} \quad (1)$$

where n is the number of peaks observed, i.e. the number of ^{13}C isotopomers corresponding to protonated carbons.

Results and discussion

Figure of merit: what is measured?

The aim of this study was to develop a new protocol for determining the ^{13}C intramolecular profile in cholesterol. In such studies, variables extracted from spectra are the molar fractions calculated from Eq. 1. Since f_i depends on the efficiency of the polarization transfer delays that are not the same for each signal, it is therefore an apparent ^{13}C abundance that is measured [27]. While a very good precision (a few permil) is mandatory, trueness is not an issue. To retrieve the true isotopic compositions, suitable correction factors should be determined by comparing values from classical irm-^{13}C NMR and from HSQC analyses of a reference sample of the given molecule. This correction was not done in this work.

Measurement precision for each position i of the cholesterol molecule was evaluated using as a parameter the relative standard deviation (RSD), expressed in ‰. RSD was calculated over the nine values obtained from each measurement for each of the 23 carbon positions measured by HSQC (24 protonated carbons but two of them, C7 and C8, had the same chemical shift). During the optimization of acquisition and processing conditions, the following repeatability parameters were used: the minimum RSD (RSD^{min}), the maximum RSD (RSD^{max}), and the mean RSD (RSD^{mean}). Minimum, maximum, and mean values of RSD were calculated over the 23 observed carbon positions. Aiming to evaluate measurement precision in an actual situation, cholesterol was extracted from cheese samples and analyzed using the same method.

Sequence optimization

HSQC is a proton-detected two-dimensional (2D) NMR experiment widely used by chemists and biochemists to elucidate molecular structures [45]. Its basic form is not performant enough to reach the permil precision required. Modifications and adjustments were necessary. The HSQC sequence with perfect symmetry in the RF pulse scheme was previously

developed by our team to improve the repeatability in olive oil authentication [28] (see the previous HSQC sequence in ESM Fig. S2). However, in that work, RF pulses were not adiabatic. Adiabatic pulses have proven to increase the accuracy of the ^{13}C NMR measurements [43], but since imperfection in 90° pulses has no influence on relative measurements [46], only the 180° hard pulses were replaced by adiabatic pulses [44]. Simple adiabatic pulses are ideal for producing inversion pulses, yet given the frequency sweep during the pulse, they induce additional phase dispersion and the transverse magnetization position after the pulse is then not symmetrical with respect to its position before the pulse. With composite adiabatic pulses, however, phase variations induced by the different components compensate each other. For this reason, these pulses are suitable for refocusing. The HSQC pulse sequence optimized in this study is presented in Fig. 2.

Other optimizations were achieved by Farjon et al. with the use of NUS, VRT, and pure shift [35]. However, their goal was to reduce the acquisition time without loss of trueness, seeking determination of absolute concentrations in mixtures of metabolites. Furthermore, the HSQC sequence and RF pulse shapes were different. While our results can be compared to those of this study, the selection criterion was different, so do the optimal conditions and the conclusion.

Parameter optimization

Spectral width and offset in dimension 1

The spectral aliasing approach (Fig. 1) reduces the number of needed acquisition points by reducing the spectral width, which induces a reduction of acquisition time [47]. Furthermore, spectral aliasing does not affect the quantitativity [48].

To observe the complete spectrum of cholesterol without signal overlap, the offsets were set to 4 ppm and 38.5 ppm with a spectral window of 12 ppm and 7.99 ppm for dimensions 1 (^{1}H) and 2 (^{13}C), respectively.

By reducing the spectral width in the ^{13}C dimension from 120 to 12 ppm, the number of t_1 increments in the ^{13}C dimension, and consequently the experimental time, was divided by 10.

Variable recycling times

The second approach that we used to reduce the experimental time was the VRT method. The principle of this method is to incrementally reduce the recovery time during the sampling of the indirect dimension [38]. The recovery time is therefore composed of two durations: τ_f which is a constant value and τ_v which is a variable (see Fig. 2 and ESM Table S1). At the first scan, the sum of τ_f and τ_v was equal to 10 s, equivalent to 7 times T_1^{max} ^{1}H. This duration affects the amplitude of the FID, therefore the values of peak integrals. The constant value of *TR* used in a regular acquisition is then replaced by a list of values (for the τ_v part of TR) that decrease when t_1 increases, which allows the reduction of the experimental time (i.e. from 1 h 32 to 42 min).

Furthermore, the use of VRT improved repeatability of f_i measurements as demonstrated by the lower values of RSD^{min}, RSD^{max}, and RSD^{mean} (see Fig. 3a and ESM Table S2).

This is consistent with results obtained from changing scan number (see "Scan number") and with previous studies where a correlation between *RSD* and experimental time was observed [28, 49–52]. Short experiments are less sensitive to spectrometer instabilities and show a better repeatability.

As shown in Fig. 2, the repetition time (*TR*) is constituted by the pulse sequence duration, which is on the order of a few milliseconds, by the acquisition time (AQ), and by τ_f and τ_v, which durations are of the order of tens or hundreds of

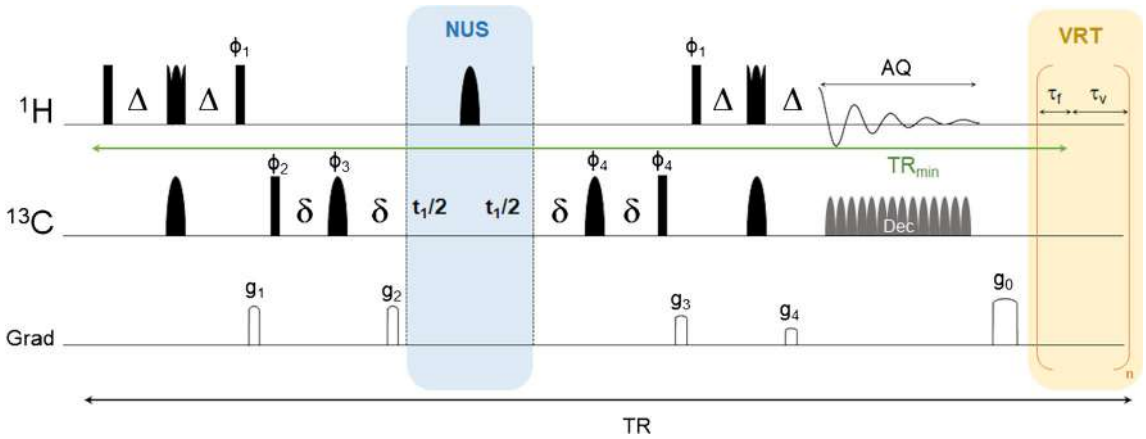

Fig. 2 Symmetrized adiabatic HSQC pulse sequence with the use of NUS (blue area, middle) and VRT (yellow area, right). ^{1}H and ^{13}C 180° adiabatic inversion pulses, adiabatic composite refocusing, hard pulses for 90° ^{1}H and ^{13}C, and adiabatic decoupling pulses were used. Phase cycling was as follows: $\phi_1 = y$; $\phi_2 = y,-y$; $\phi_3 = x$; $\phi_4 = x,-x$. Δ was set to 2.3 ms and δ was set to 1 ms. τ_f and τ_v were the constant and the variable parts of the recovery time, respectively

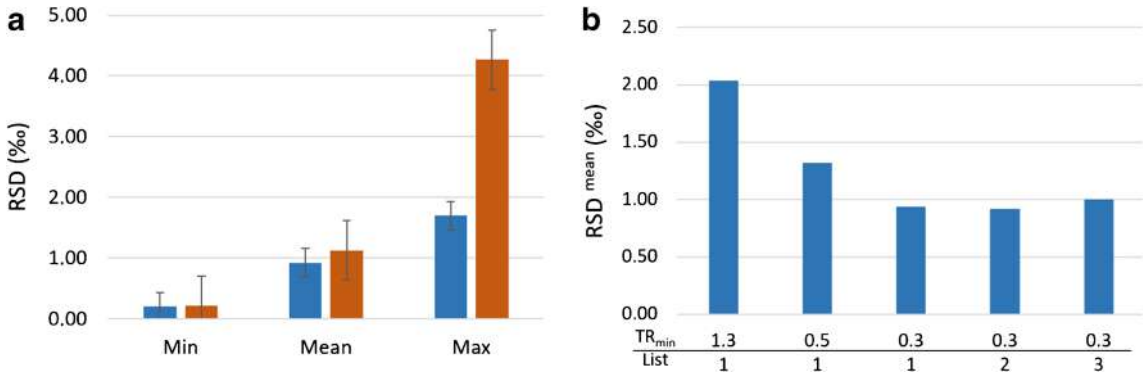

Fig. 3 **a** Minimum, maximum, and mean values of f_i *RSD* (‰) with VRT in 42 min (blue, left) and without VRT in 1 h 32 min (orange, right). **b** Influence of the minimum repetition time and of the shape of the τ_v list on RSD^{mean} (‰)

milliseconds. The minimum value of the repetition time (TR^{min}) is therefore essentially composed by AQ plus τ_f. Moreover, the final experimental time depends on TR^{min} and on the shape of the function used to define τ_v. We have therefore evaluated the influence of this shape and of the value of TR^{min} on the *RSD* values.

Three shapes of τ_v (see ESM Fig. S4) and different values of TR^{min}, i.e. 1.3, 0.5, and 0.3 s were tested (see ESM Table S3). RSD^{mean} evolved in the same way as TR^{min} (see Fig. 3b). A value less than 1‰ was obtained for RSD^{mean} with 0.2 s for τ_f and 0.1 s for AQ. However, no significant difference was observed between the three shapes of τ_v. For further optimization, the list 2 with $TR^{min} = 0.3$ s was used because it had the smallest average *RSD* values. This list induced a reduction of the experimental time by 2.2. The value of 0.2 s for τ_f is the minimum value allowed by our spectrometer, and AQ values lower than 0.1 s induce truncation artefacts.

NUS and/or LP

In order to further speed up the acquisition, non-uniform sampling (NUS) and linear prediction (LP) were tested. NUS methods substitute non-uniformly experimental points of the FID by calculated points, whereas LP adds calculated points at the end of the experimental ones. In both cases, the number of acquired points is the same but calculated points are in different places in the FID and the reconstruction algorithm is not the same. Consequently, effects of these two methods on f_i *RSD* are different (see Fig. 4 and ESM Table S4).

Experiments were acquired with a total number of FID points equal to 512, therefore with 256 points acquired for NUS or LP 50% and 128 for NUS or LP 25%. No significant differences were observed in RSD^{min} and RSD^{mean} values between NUS (50 or 25%) and LP (50 or 25%). However, RSD^{max} was the discriminant criterion: RSD^{max} was 1.3 times higher for LP than for NUS due to the imperfect repartition of the theoretical points.

It was possible to reduce experimental time by increasing the percentage of calculated points in order to decrease the number of acquired points, but our results showed that RSD^{max} was 2 times higher for 25% than for 50% (NUS or LP, see Fig. 4). This result could be explained by a too low number of experimental points, 128 points compared to 256 points.

Hence, NUS 50% was chosen, which corresponds to an additional reduction of the experiment time by a factor of 2.

Another experiment with 256 points acquired was performed using a combination of NUS and LP in order to reach 1024 final FID points. The results presented higher RSD^{min}, RSD^{mean}, and RSD^{max} values, probably because the number of theoretical points was lower than the number of experimental points compared to NUS 50%.

NUS algorithms

For data reconstruction, two NUS algorithms were used: iteratively reweighted least squares (IRLS) and iterative shrinkage/thresholding (IST). The latter is implemented in the TopSpin software without an additional charge and is used by default during 2D processing. The IRLS algorithm is a more recent algorithm that activates a "virtual echo" parameter that is known to slightly improve the 2D treatment in spectral applications. However, this algorithm is not free of charge, the processing is significantly longer, and before the work presented here, it was never used for very high-precision measurements. We have therefore evaluated the impact of the two algorithms on precision in order to optimize the data processing.

Figure 5a (ESM Table S5) shows the *RSD* values obtained on the same spectra with the 2 algorithms. A better precision was observed with the IST algorithm. In fact, this algorithm allowed having more repeatable signals with less interference on all the carbon positions of the cholesterol molecule as illustrated for C6 represented in Fig. 5b. RSD^{max} obtained using the IRLS algorithm was around 8‰, whereas with the IST

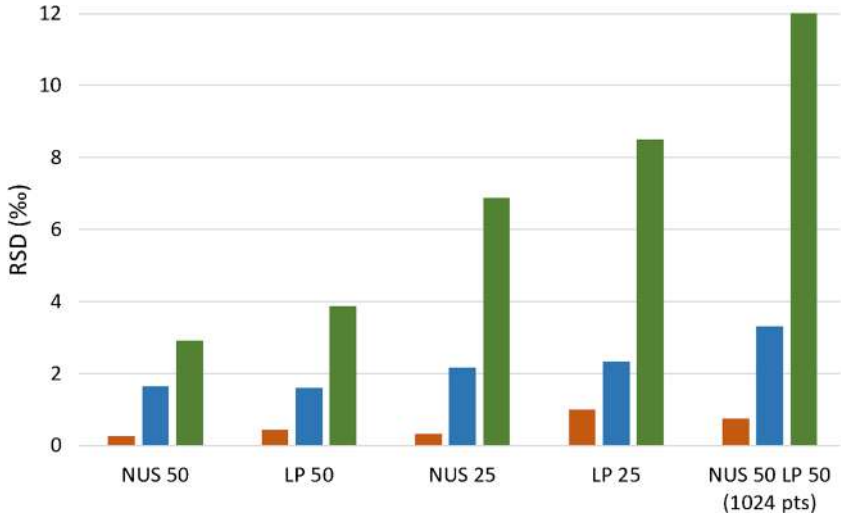

Fig. 4 RSD^{min} (orange, left), RSD^{mean} (blue, middle), and RSD^{max} (green, right) in ‰ for different NUS and LP conditions (512 points treated)

algorithm, it was less than 5‰. Moreover, treatments with IRLS took 3 times longer than with the IST algorithm for the same number of points. The IST algorithm seems therefore a better choice for our application and was retained for this study.

This is not surprising, giving the results of the well-known NUScon competition organized by the NMRBox team at the University of Connecticut (https://nmrbox.org/). Neither IST nor IRLS won the competition, suggesting that Bruker CS reconstruction methods are not optimal when the data gets sparse. More efficient algorithms will be tested in the future; however, in this work, we were focused on performances that can be obtained using commercial hardware and software.

Spectral calibration

In this study, the results were processed by two operators. In the initial processing strategy, five spectra were recorded per session in order to assess the repeatability of the measurements. However, due to variation in the spectral calibration between operators, significantly different integrals and *RSD* values were obtained. This variation probably comes from the lower digital resolution in the ^{13}C dimension. In order to take into account the influence of eventual calibration shift, three spectra were recorded for each acquisition and each spectrum was processed three times (including calibration). With this protocol, no significant difference was observed between the two operators.

Scan number

The sequence has been tested with a NS of 2, 4, and 8. The results showed no variation in precision with the number of scans on the RSD^{min} and RSD^{mean}, but a higher RSD^{max} for 8 scans was obtained (see Fig. 6a and ESM Table S6). Therefore, the number of scans adopted was set to 2. In these experimental conditions, NS seems not to be the limiting factor and increasing it cannot induce a further reduction in *RSD* values. Once again, we observed here the impact of experimental time on RSD; long experiments are more sensitive to

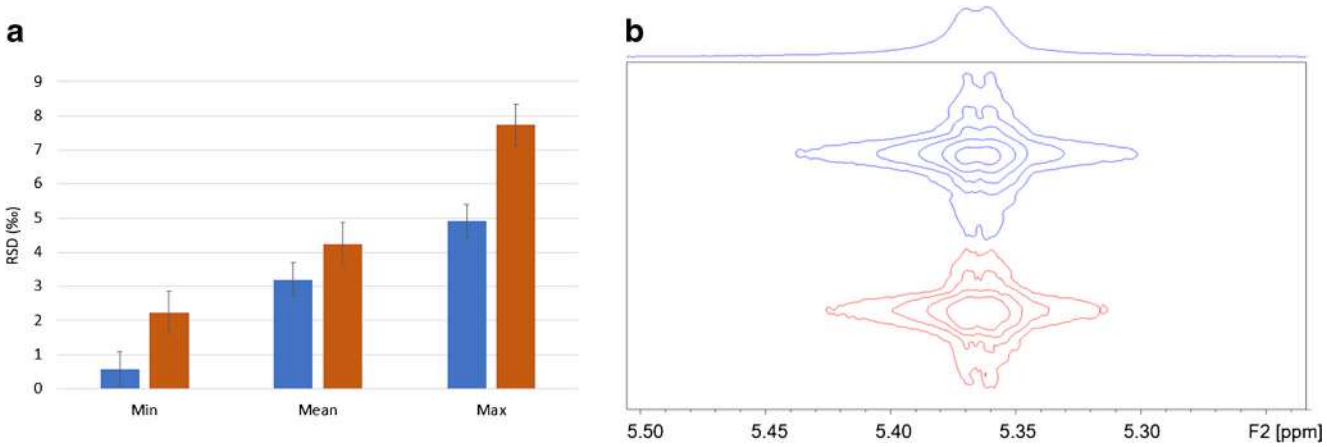

Fig. 5 **a** RSD^{min}, RSD^{mean}, and RSD^{max} (‰) with the IST (blue, left) and IRLS (orange, right) algorithm. **b** C6 signal treated with IST (red, lower) and IRLS (blue, upper)

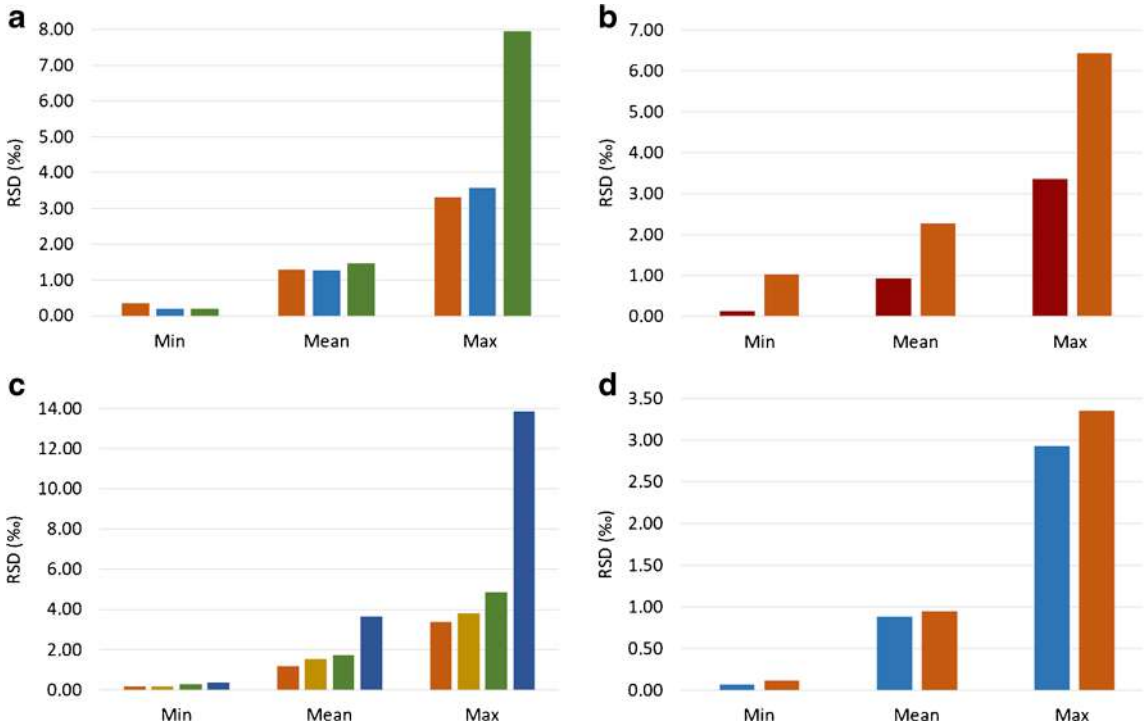

Fig. 6 RSD^{min}, RSD^{mean}, and RSD^{max} (‰) **a** with NS = 2 (orange, left), NS = 4 (blue, middle), and NS = 8 (green, right); **b** without pure-shift fragment (red, left) and with pure-shift fragment (orange, right); **c** with 20 mg (orange, left), 15 mg (yellow, middle left), 10 mg (green, middle right), and 5 mg (blue, right); and **d** with 40 mg of cholesterol in a Shigemi tube (blue, left) and 80 mg of cholesterol in a standard tube (orange, right)

spectrometer instabilities in the course of time, leading to an increase of RSD, while short experiments are less sensitive to such instabilities and show a better precision, as long as the SNR and the resolution are sufficient to quantify relevant peaks with the target precision [28, 49–52]. This observation seems strange taking into account the good stability of modern-day spectrometers, but readers have to keep in mind that the precision targeted in this work is currently the limit of such spectrometers.

Pure shift

In the Farjon et al. study, the pulse sequence included a pure-shift segment that increased resolution by supressing the splitting due to ^{1}H-^{1}H coupling [35]. The pure shift segment was therefore tested on our sequence. However, the results showed higher *RSD* values than without the pure-shift segment (see Fig. 6b and ESM Table S7), probably because in this case the sampling period is separated in several chunks with imperfect phase coherence between them (see ESM Fig. S3).

Cholesterol concentration

Optimizations described in the previous sections were done with 20 mg of cholesterol in the tube. Effect of concentration was then investigated in order to determine the minimum quantity of cholesterol that can be analyzed while maintaining a precision of few permil. It was possible to analyze 10 mg of cholesterol using a standard 5-mm NMR tube with very satisfactory results (see Fig. 6c and ESM Table S8).

It must be noted that an additional reduction in the amount of the analyzed compound can be obtained by using a volume-reduced tube such as the Shigemi tube. Our results showed that with such a tube, 5 mg of cholesterol (half the quantity used with a standard NMR tube) was sufficient while keeping all other parameters unchanged (see Fig. 6d and ESM able S9).

Application to cholesterol extracted from cheese samples

Aiming to test the applicability of the developed method to cholesterol extracted from biological matrices, four cheese samples were considered in this study. Cholesterol extracted from these samples was analyzed using the same HSQC sequence with the best set of parameters determined with commercial cholesterol. *RSD* values were determined for all carbon positions measured over the 4 cheese samples (22 values were obtained instead of 23 since C14 and C17 signals were overlapped). *RSD* values for each sample as well as pooled *RSD* values from all samples (see Table 1) showed excellent precision over the whole set of carbon positions. Pooled RSD^{min}, pooled RSD^{max}, and pooled RSD^{mean} were 0.79, 2.33, and 1.36‰, respectively.

Table 1 *RSD* of molar fractions (f_i) of cholesterol from cheese samples

Variable[a]	*RSD* of f_i (‰)[b]				Pooled *RSD* (‰)[c]
	Sample 1	Sample 2	Sample 3	Sample 4	
C18	0.62	1.01	0.83	0.78	0.82
C21	0.76	0.13	1.29	0.82	0.86
C19	0.86	0.83	0.84	0.62	0.79
C11	1.30	0.74	1.50	1.03	1.18
C26	0.71	0.54	0.55	2.01	1.13
C27	0.77	1.37	0.44	0.90	0.93
C23	1.18	1.13	0.46	0.64	0.91
C15	1.01	1.72	1.71	0.72	1.36
C25	3.23	2.01	0.73	2.57	2.33
C16	0.61	1.41	2.13	2.64	1.86
C2	2.72	0.38	1.15	0.88	1.55
C7/C8	0.50	0.29	2.04	1.34	1.25
C20	0.78	2.30	3.10	1.69	2.15
C22	0.57	1.25	1.38	0.84	1.06
C1	1.28	1.14	1.27	0.51	1.09
C24	2.29	2.78	1.15	2.29	2.21
C12	1.05	2.46	1.00	1.05	1.52
C4	1.10	0.34	1.67	1.11	1.16
C9	1.83	3.22	0.67	2.03	2.14
C14/C17	1.81	1.32	1.63	1.48	1.57
C3	0.63	0.92	0.80	1.29	0.94
C6	1.45	1.38	0.70	0.63	1.10

[a] See Fig. 1 for variable labelling

[b] *RSD* of f_i for each sample were calculated using values obtained from 3 spectra with 3 treatments per spectrum

[c] Pooled *RSD* values were calculated over the *RSD* sets of the 4 samples

Conclusion

A symmetric adiabatic 2D HSQC pulse sequence has been developed for the first time for ^{13}C isotopomics in low quantities of cholesterol with high precision. While 5 mg represents a usual amount in the NMR analysis, it is a real challenge when very high precision (permil) and small experimental time are targeted, especially for the quantitation of heteronuclei as ^{13}C isotopomers. Folding of the peaks was used to shorten the acquisition time, and each spectrum was treated three times in order to eliminate errors related to calibration. Furthermore, NUS and VRT were also optimized to shorten the acquisition time. Influences of the scan number and of a pure shift strategy were also tested. The method was developed on a system with a cryogenically cooled probe and was not tested on a room-temperature system.

Moreover, with this methodology and using a Shigemi tube, only 5 mg of cholesterol is needed to reach an *RSD* of a few permil. For most of the detected peaks, *RSD* is below 3 permil (10 carbons have an *RSD* below 1 permil, 7 carbons between 1 and 3 permil, and 6 carbons present an *RSD* between 3 and 5 permil). These results were obtained with an experimental time of only 31 min per spectrum while an INEPT spectrum would have taken 16.2 h for the same amount of cholesterol, therefore more than 31 times longer.

The optimized method was then tested on cholesterol extracted from cheese samples. Excellent precision, of the same magnitude as with commercial cholesterol, was observed on all carbon positions of the molecule.

Finally, the new developed methodology described herein can find widespread use in isotopomics of biomolecules—such as sterols, glucose, amino acids, and their derivatives—with applications in medical investigations and food authentication.

Supplementary Information The online version contains supplementary material available at https://doi.org/10.1007/s00216-020-03135-0.

Acknowledgements The CORSAIRE platform from Biogenouest is acknowledged. The authors are grateful to Dr. Jonathan Farjon for *his* help in implementing NUS in the adiabatic HSQC sequence.

Code availability Not applicable

Authors' contributions Lenny Haddad: investigation, data curation, formal analysis, writing—original draft; Sophie Renou: investigation, data curation, formal analysis, writing—original draft; Gérald S. Remaud: conceptualization, resources, supervision, writing—review and editing, funding acquisition; Toufic Rizk: project administration, funding acquisition; Joseph Bejjani: conceptualization, supervision, resources, writing—review and editing, funding acquisition; Serge Akoka: conceptualization, methodology, supervision, writing—review and editing

Funding L.H. received financial support from the Research Council of Saint-Joseph University of Beirut and CEISAM. S.R. received financial support from the French Research Ministry. The authors received funding from the Région Pays de la Loire (Grant RFI-Food 4.2-Project AIMM).

Data availability Not applicable

Compliance with ethical standards

Conflict of interest The authors declare that they have no competing interests.

References

1. Röhrl C, Stangl H. Cholesterol metabolism - physiological regulation and pathophysiological deregulation by the endoplasmic reticulum. Wien Med Wochenschr. 2018;168:280–5.
2. Kanungo S, Soares N, He M, Steiner RD. Sterol metabolism disorders and neurodevelopment-an update. Dev Disabil Res Rev. 2013;17:197–210.
3. Gidding SS, Allen NB. Cholesterol and atherosclerotic cardiovascular disease: a lifelong problem. JAHA. 2019;8:1–3.
4. Hellman L, Rosenfeld RS, Eidinoff ML, Fukushima DK, Gallagher TF, Wang CI, et al. Isotopic studies of plasma cholesterol of endogenous and exogenous origins. J Clin Invest. 1955;34:48–60.
5. Atkinson A, Colburn W, DeGruttola V, Demets D, Downing G. Biomarkers and surrogate endpoints: preferred definitions and conceptual framework. Clin Pharmacol Ther. 2001;69:89–95.
6. Martins-de-Souza D. Is the word 'biomarker' being properly used by proteomics research in neuroscience? Eur Arch Psychiatry Clin Neurosci. 2010;260:561–2.
7. Koal T, Schmiederer D, Pham-Tuan H, Röhring C, Rauh M. Standardized LC-MS/MS based steroid hormone profile-analysis. J Steroid Biochem Mol Biol. 2012;129:129–38.
8. Erich S, Schill S, Annweiler E, Waiblinger H-U, Kuballa T, Lachenmeier DW, et al. Combined chemometric analysis of (1)H NMR, (13)C NMR and stable isotope data to differentiate organic and conventional milk. Food Chem. 2015;188:1–7.
9. Coplen TB. Guidelines and recommended terms for expression of stable-isotope-ratio and gas-ratio measurement results: guidelines and recommended terms for expressing stable isotope results. Rapid Commun Mass Spectrom. 2011;25:2538–60.
10. Stott AW, Evershed RP. $\delta^{13}C$ analysis of cholesterol preserved in archaeological bones and teeth. Anal Chem. 1996;68:4402–8.
11. Mendelsohn D, Immelman AR, Vogel JC, Chevallerie GVL. Carbon-13 in natural cholesterol. Biomed Environ Mass Spectrom. 1986;13:21–4.
12. Muccio Z, Jackson GP. Isotope ratio mass spectrometry. Analyst. 2009;134:213–22.
13. Hayes JM. Fractionation of carbon and hydrogen isotopes in biosynthetic processes. Rev Mineral Geochem. 2001;43:225–77.
14. Gauchotte-Lindsay C, Turnbull SM. On-line high-precision carbon position-specific stable isotope analysis: a review. TrAC Trends Anal Chem. 2016;76:115–25.
15. Wuerfel O, Greule M, Keppler F, Jochmann MA, Schmidt TC. Position-specific isotope analysis of the methyl group carbon in methylcobalamin for the investigation of biomethylation processes. Anal Bioanal Chem. 2013;405:2833–41.
16. Rossmann A, Butzenlechner M, Schmidt H-L. Evidence for a nonstatistical carbon isotope distribution in natural glucose. Plant Physiol. 1991;96:609–14.
17. Eiler J, Cesar J, Chimiak L, Dallas B, Grice K, Griep-Raming J, et al. Analysis of molecular isotopic structures at high precision and accuracy by Orbitrap mass spectrometry. Int J Mass Spectrom. 2017;422:126–42.
18. Neubauer C, Sweredoski MJ, Moradian A, Newman DK, Robins RJ, Eiler JM. Scanning the isotopic structure of molecules by tandem mass spectrometry. Int J Mass Spectrom. 2018;434:276–86.
19. Eiler JM. The isotopic anatomies of molecules and minerals. Annu Rev Earth Planet Sci. 2013;41:411–41.
20. Neubauer C, Crémière A, Wang XT, Thiagarajan N, Sessions AL, Adkins JF, et al. Stable isotope analysis of intact oxyanions using electrospray quadrupole-Orbitrap mass spectrometry. Anal Chem. 2020;92:3077–85.
21. Remaud GS, Giraudeau P, Lesot P, Akoka S. Isotope ratio monitoring by NMR. Part 1: Recent advances. In: Webb GA, editor. Modern magnetic resonance. Cham: Springer International Publishing; 2016. p. 1–26.
22. Martin GJ, Zhang BL, Martin ML, Dupuy P. Application of quantitative deuterium NMR to the study of isotope fractionation in the conversion of saccharides to ethanols. Biochem Biophys Res Commun. 1983;111:890–6.
23. Martin GJ, Guillou C, Martin ML, Cabanis MT, Tep Y, Aerny J. Natural factors of isotope fractionation and the characterization of wines. J Agric Food Chem. 1988;36:316–22.
24. Caytan E, Botosoa EP, Silvestre V, Robins RJ, Akoka S, Remaud GS. Accurate quantitative 13C NMR spectroscopy: repeatability over time of site-specific 13C isotope ratio determination. Anal Chem. 2007;79:8266–9.
25. Guyader S, Thomas F, Jamin E, Grand M, Akoka S, Silvestre V, et al. Combination of 13C and 2H SNIF-NMR isotopic fingerprints of vanillin to control its precursors. Flavour Fragr J. 2019;34:133–44.
26. Liu C, McGovern GP, Liu P, Zhao H, Horita J. Position-specific carbon and hydrogen isotopic compositions of propane from natural gases with quantitative NMR. Chem Geol. 2018;491:14–26.
27. Akoka S, Remaud GS. NMR-based isotopic and isotopomic analysis. Prog Nucl Magn Reson Spectrosc. 2020;120–121:1–24.
28. Merchak N, Silvestre V, Rouger L, Giraudeau P, Rizk T, Bejjani J, et al. Precise and rapid isotopomic analysis by 1H–13C 2D NMR: application to triacylglycerol matrices. Talanta. 2016;156–157:239–44.
29. Hajjar G, Rizk T, Akoka S, Bejjani J. Cholesterol, a powerful 13C isotopic biomarker. Anal Chim Acta. 2019;1089:115–22.
30. Caytan E, Remaud GS, Tenailleau E, Akoka S. Precise and accurate quantitative 13C NMR with reduced experimental time. Talanta. 2007;71:1016–21.
31. Jézéquel T, Joubert V, Giraudeau P, Remaud GS, Akoka S. The new face of isotopic NMR at natural abundance: the new face of isotopic NMR at natural abundance. Magn Reson Chem. 2017;55:77–90.
32. Jim S, Ambrose SH, Evershed RP. Stable carbon isotopic evidence for differences in the dietary origin of bone cholesterol, collagen and apatite: implications for their use in palaeodietary reconstruction. Geochim Cosmochim Acta. 2004;68:61–72.
33. Laffey AO, Krigbaum J, Zimmerman AR. A protocol for pressurized liquid extraction and processing methods to isolate modern and

ancient bone cholesterol for compound-specific stable isotope analysis. Rapid Commun Mass Spectrom. 2017;31:235–44.
34. Hoffman DW, Rasmussen C. Position-specific carbon stable isotope ratios by proton NMR spectroscopy. Anal Chem. 2019;91:15661–9.
35. Farjon J, Milande C, Martineau E, Akoka S, Giraudeau P. The FAQUIRE Approach: FAst, QUantitative, hIghly Resolved and sEnsitivity Enhanced ^{1}H, ^{13}C Data. Anal Chem. 2018;90:1845–51.
36. Marchand J, Martineau E, Guitton Y, Dervilly-Pinel G, Giraudeau P. Multidimensional NMR approaches towards highly resolved, sensitive and high-throughput quantitative metabolomics. Curr Opin Biotechnol. 2017;43:49–55.
37. Merchak N, El Bacha E, Bou Khouzam R, Rizk T, Akoka S, Bejjani J. Geoclimatic, morphological, and temporal effects on Lebanese olive oils composition and classification: a (1)H NMR metabolomic study. Food Chem. 2017;217:379–88.
38. Macura S. Accelerated multidimensional NMR data acquisition by varying the pulse sequence repetition time. J Am Chem Soc. 2009;131:9606–7.
39. Korzhneva DM, Ibraghimov IV, Billeter M, Orekhov VY. MUNIN: application of three-way decomposition to the analysis of heteronuclear NMR relaxation data. J Biomol NMR. 2001;21:263–8.
40. Barkhuijsen H, de Beer R, Bovée WMMJ, van Ormondt D. Retrieval of frequencies, amplitudes, damping factors, and phases from time-domain signals using a linear least-squares procedure. J Magn Reson (1969). 1985;61:465–81.
41. Barna JCJ, Laue ED, Mayger MR, Skilling J, Worrall SJP. Exponential sampling, an alternative method for sampling in two-dimensional NMR experiments. J Magn Reson. 1987;73:69–77.
42. Srivastava NK, Pradhan S, Gowda GAN, Kumar R. In vitro, high-resolution 1H and 31P NMR based analysis of the lipid components in the tissue, serum, and CSF of the patients with primary brain tumors: one possible diagnostic view. NMR Biomed. 2010;23:113–22.
43. Tenailleau E, Akoka S. Adiabatic 1H decoupling scheme for very accurate intensity measurements in 13C NMR. J Magn Reson. 2007;185:50–8.
44. Thibaudeau C, Remaud G, Silvestre V, Akoka S. Performance evaluation of quantitative adiabatic 13C NMR pulse sequences for site-specific isotopic measurements. Anal Chem. 2010;82:5582–90.
45. Castañar L, Parella T. Chapter Four - Recent advances in small molecule NMR: improved HSQC and HSQMBC experiments. In: Webb GA, editor. Annual reports on NMR spectroscopy: Academic Press; 2015. p. 163–232.
46. Karabulut N, Baguet E, Trierweiler M, Akoka S. Improvement in quantitative accuracy of 13C DEPT integrals by parameter-optimization. Anal Lett. 2002;35:2549–63.
47. Foroozandeh M, Jeannerat D. Reconstruction of full high-resolution HSQC using signal split in aliased spectra: reconstruction of full high-resolution spectra from aliased spectra. Magn Reson Chem. 2015;53:894–900.
48. Rouger L. Development and evaluation of fast methods in multidimensional NMR for the characterization of elastomeric mixtures. Thesis, Nantes. 2007. http://www.theses.fr/2017NANT4073. Accessed 7 April 2020.
49. Silvestre V, Goupry S, Trierweiler M, Robins R, Akoka S. Determination of substrate and product concentrations in lactic acid bacterial fermentations by proton NMR using the ERETIC method. Anal Chem. 2001;73:1862–8.
50. Giraudeau P, Guignard N, Hillion E, Baguet E, Akoka S. Optimization of homonuclear 2D NMR for fast quantitative analysis: application to tropine–nortropine mixtures. J Pharmaceut Biomed Anal. 2007;43:1243–8.
51. Martineau E, Giraudeau P, Tea I, Akoka S. Fast and precise quantitative analysis of metabolic mixtures by 2D 1H INADEQUATE NMR. J Pharmaceut Biomed Anal. 2011;54:252–7.
52. Martineau E, Akoka S, Boisseau R, Delanoue B, Giraudeau P. Fast quantitative ^{1}H– ^{13}C two-dimensional NMR with very high precision. Anal Chem. 2013;85:4777–83.

Lenny Haddad is a PhD student under joint supervision between Saint-Joseph University of Beirut and the University of Nantes. She is currently working on the characterization and authentication of dairy products with high-resolution metabolomic and isotopomic profiling using nuclear magnetic resonance (NMR) spectroscopy.

Sophie Renou is a PhD student at Nantes University. An analytical chemist by education, she is now working on the development of new NMR pulse sequences for ^{13}C isotopic analysis.

Gérald S. Remaud was recruited in 2003 as Professor at the University of Nantes, after spending 11 years at EUROFINS Laboratory (Nantes, France) as Technical Director. His research areas cover quantitative NMR methodologies, especially isotopic ^{13}C NMR and its application to the investigation of isotopic affiliation.

Joseph Bejjani is Associate Professor at Saint Joseph University of Beirut – Faculty of Sciences. He has a background in organic and organometallic chemistry with application in asymmetric synthesis. His current research focuses on the development of isotopomic, lipidomic, and metabolomic methods using NMR spectroscopy for the identification of biomarkers mainly for food authentication and medical applications.

Toufic Rizk is Full Professor at Saint Joseph University of Beirut. He is an international expert in food safety and was notably Head of the Center of Research and Analysis of the Faculty of Sciences and Dean of the same Faculty at Saint Joseph University. His current research deals with food safety and food authenticity.

Serge Akoka is Full Professor of Analytical Chemistry at the University of Nantes and works in the research unit CEISAM (*Chimie Et Interdisciplinarité, Synthèse, Analyse, Modélisation*). His current research interests are as follows: (i) isotopic analysis by NMR at natural abundance; (ii) methodological developments in quantitative NMR, adiabatic RF pulses for high-precision ^{13}C-NMR, quantitative 2D NMR.